Technische Universität München
Lehrstuhl für Kommunikationsnetze
Prof. Dr.-Ing. Wolfgang Kellerer

Bachelor's Thesis

Title of the Thesis

Author:	Buitrago Méndez, Arturo
Address:	Türkenstrasse 58a
	80799 München
	Germany
Matriculation Number:	03646899
Supervisor:	Supervisor Name
Begin:	01. January 1900
End:	01. January 2000

With my signature below, I assert that the work in this thesis has been composed by myself independently and no source materials or aids other than those mentioned in the thesis have been used.

München, 11.06.2014

Place, Date

Signature

München, 11.06.2014

Place, Date

Signature

Kurzfassung

A short abstract of the thesis in German.

Abstract

A short abstract of the thesis in English.

Contents

Chapter 1

Introduction

One of the most promising directions the field of communication networks has explored in the last years has been the Internet of Things (IoT). An explosion in the capability of everyday objects to connect and communicate with each other via wireless networks promises to mightily expand the boundaries hitherto explored by technology. It also promises to place an almost unmanageable amount of stress into the technologies and infrastructure already in place.

One of the proposed approaches to ameliorate the overload of connections originating from hundreds of devices to a base station is the grouping of the signals via different algorithms into clusters, which then transmit the aggregated information in one single signal to the rest of the network.

Although many such algorithms have been proposed, especially coming from the field of Wireless Sensor Networks (WSNs) where data aggregation is much more a matter of course, there has been woefully little attention payed to the viability of such mechanisms in comparison to one another in a scenario conforming to the standards and circumstances of LTE-A and Device to Device (D2D) communication. These kind of considerations are specially relevant when considering the prospective arrival of the IoT, the emergence of concepts such as smart grids and smart cities and the prospect of 5G as the next generation of technology that will have to deal with these issues.

This thesis aims to do just that: present a coherent and realistic simulation scenario for the clustering of devices within LTE-A, with special attention payed to the interference caused by the simultaneous transmission of information, both within the clusters and between other clusters. This will allow a fair comparison of existing clustering schemes and the degree to which they effectively alleviate congestion in the network.

The main part of the thesis will first present the background of the topic, explaining the difficulties arising from an increase in network-capable devices to the limits posed by the Random Access Procedure in place at the moment. The trade-offs of clustering will be explored, along with an enumeration of some of the most importants algorithms taken into account in this work. This chapter will also give an overview of the factors that need to be contemplated during the simulation of the network, along with the motivation for the choice of the simulation environment. Additionaly, justification will be given for the metrics used for evaluating the results of the clustering algorithms.

Next, the implementations of said simulations will be explored. This chapter will delve deeper into the details of bringing the theoretical models into the code used, with a more in-depth discussion of the decisions taken when finalizing the constraints under which the tests were run. The results that they yield will then be discussed and evaluated in the subsequent chapter, with especial attention payed to a direct comparison of the performance of different clustering algorithms. Finally, a discussion of the results will identify the ones most promising for future research and further development.

Chapter 2

Background

2.1 Random Access and its Limitations

The necessity of the expansion of the existing standards of wireless networks for the effective handling of large numbers of Machine Type Communications (MTC) had already been identified by the 3GPP early in the implementation of Long Term Evolution (LTE) as a standard in [3rd11]. As explained in [LAAZ14], a large amount of problems arise with increasingly large amounts of devices connecting to the Base Station (BS) or Evolved Node B (eNodeB) mostly due to the Random Access (RA) procedure that has to be initiated with every connection.

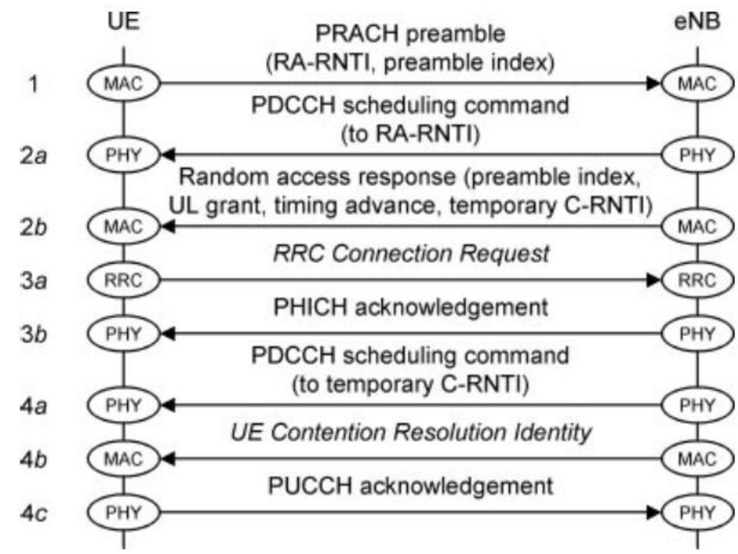

Figure 2.1: Detail of the Random Access Procedure, [Cox12]

RA procedures occurr when a device intends to utilize resources on the Physical Uplink Shared Channel (PUSCH), but has not been given access to the Physical Uplink Control Channel (PUCCH) by the appropriate eNB, which is needed for a scheduling request. As described in [Cox12], the User Equipment (UE) then sends a random access preamble to trigger the procedure, in order to gain the desired access.

This preamble is chosen randomly from an available set generated with a Zadoff-Chu mathematical sequence and transmitted on the Physical Random Access Channel (PRACH). The eNB then solves any possible collisions that may occurr from devices transmitting with the same preamble, granting access to some while ordering others to back off for a certain amount of time. If no access grant is given after several tries, the transmission is considered to have failed.

When a large amount of these connections are initiated in a short time frame, the contention resolution procedures cannot deal with them in a timely manner and many of them are dropped or delayed significantly, waiting for an opportunity to synchronize with the eNodeB, as shown in [PCZZ16]. This scenario occurs most often either because the transmission times are highly correlated or just due to the large number of devices in a given area. Both of these circumstances, both in isolation and in conjunction, will be very ordinary occurences in Internet of Things (IoT) and Smart City applications.

2.2 D2D

2.3 Clustering

Many approaches have been suggested for the improvement of the circumstances described in the preceding section, as summarized succintly in [LAAZ14], mostly dealing with the improvement of the RA procedures or an expansion of the standards for the Random Access Channel (RACH). Another viable alternative, as presented in a variety of papers ([WHS12a],[LWW+14],[WSH+13],[LQL13]) is the clustering of transmitting devices. This approach aims to reutilize the coding and frequency resources within a given set of UEs for different ends, such as decreasing the load on the eNB, increasing the coverage area of the network or minimizing the power consumption of the units involved.

Clustering works by designating devices, called Cluster Heads (CH) that act as relays between the different UEs in a certain area and the eNB or a further Cluster Head by aggregating the data sent to it and relaying it. This aggregation can occur simply by gathering the data over a period of time and transmitting the same information in one long message, as in [SOIJ15], or through actual elimination of data redundancy, as contemplated in [RCCM15].

The Cluster Heads themselves are often dedicated gateways, as utilized in [NXW11] or

[SOIJ15] and have been utilized especially in Wireless Sensor Networks with some frequency. Another, very promising approach to creating clusters is the use of direct Device-to-Device (D2D) communication to eliminate the need for dedicated Cluster Heads and enable dynamic cluster forming depending on the circumstances experienced by the network.

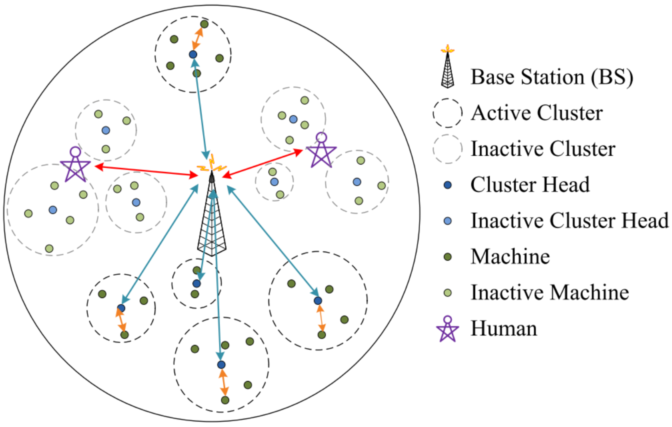

Figure 2.2: Example of D2D Clustering in a network [WSH+13]

This type of clustering scheme promises to bring much needed flexibility to the creation of these structures, since they do not necessitate much investment in additional infrastructure, nor much prior information about the density of devices. D2D communications bring many benefits, both for the user and the network, but also raise several issues that have not been yet properly investigated so far, see [KK14a]. As devices utilize the same shared resources in a constrained space, interference becomes more of an issue as devices elect to transmit their messages in the same bandwith. This topic of inter-cluster interference due to reuse of resources and its effects on possible D2D connections is of great interest to this thesis.

As mentioned earlier, this sort of application is specially intriguing in the case of highly dense Smart Cities and the IoT. Despite the promising vistas offered by this technology, there is a dearth of research concerning this specific scenario, be it a comparison of different clustering schemes or even the detailed simulation of one clustering schemes with varying parameters. Although detailed surveys of algorithms exist, such as [JYZ09] or [ATN14], they mostly center around description and classification. This thesis is meant to alleviate this lack of exploration. Not only will different clustering schemes be analyzed and compared fairly, they will also be scrutinized under different criteria, allowing for an assessment of their viability. This will hopefully give a direction to future possible research in this area, by highlighting some of them as viable or others as not viable at all.

The next chapters will explain in detail the steps taken to create the simulation environment as well as a presentation and evaluation of the results it yielded.

Chapter 3

Implementation

Pequeno rundown de como vamos a estar haciendo las varas.

For the creation of such a testing environment, four elements were recognized as of utmost importance to the validity of the tests and the author sought to implement them accordingly. In the following, they will be presented with detail, justifying the sources of the models and the parameter choices made.

The aforementioned elements are:

- Generation and distribution of UEs
- Path loss (attenuation)
- Shadow fading
- Random access procedure and interference
- Clustering algorithms

3.1 Generation and distribution of UEs

Often called a "completely" random process, a Poisson process is a process where every event is stochastically independent of all other points in it, see [Kee16]. This generation process is common in investigations about the performance of networks, as eloquently expressed by [Kee] In our case, the Poisson-distributed random variable are the number of points in the bounded region we are investigating. The distribution is described by the following probability mass function:

$$P\left(x\ points\ in\ region\right) = \frac{e^{-\lambda}\lambda^{x}}{x!} \tag{3.1}$$

By providing the λ above, often called mean density ([Kee16]), we can adjust the expected amount of points generated in a given area. In order to evaluate the robustness of different algorithms, the tests were made with a variety of λ values. The generated amount of points are then distributed in the given area with a uniform distribution, where both the x and y value are distributed along the appropriate axis. In both cases, the *Python* package *NumPy* was utilized for the realization of the random distributions.

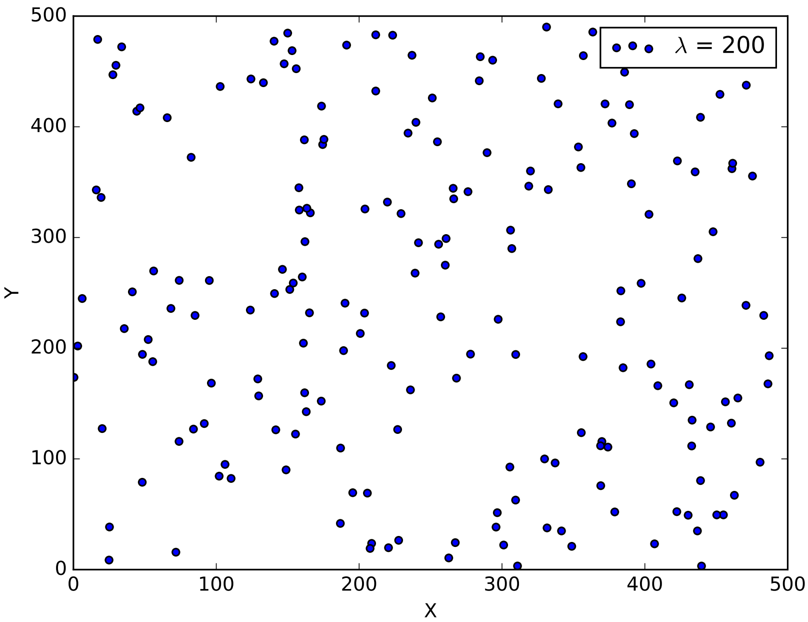

Figure 3.1: Example of a PPP with $\lambda = 200$

Thus we have generated the number and position of all our UEs according to a Poisson point process (PPP).

3.2 Path loss (attenuation)

Whenever transmission between devices is being investigated, loss due to attenuation as the signal propagates through space is an unavoidable topic. Distance degrades electromagnetic waves in terms of power in any real system and any simulation that does not reflect this phenomenon is simply not valid.

In search of the best documented and most forward-looking models available, we settled on the use of METIS (Mobile and wireless communications Enablers for the Twenty-twenty Information Society), a EU Project that seeks to promote the definition of 5G mobile technologies. Its channel model, presented in its deliverables ([Mw15]) was especially insightful.

For the purposes of this thesis, the Stochastic Model, a "geometry-based stochastic channel model", was chosen for the way it lined up with our own goals, especially when it came to level of detail and complexity. Their figures are based on previous efforts by 3GPP studies to model these same phenomena. Due to the highly dense, urban system we are investigating, propagation scenario number one, "Urban Micro" was selected. Due to the constraints of this thesis, we narrowed our focus on Outside-to-Outside (020) connections, although the integration of Outside-to-Inside (O2I) could be a feature of future research.

When calculating the attenuation for a given path between two devices, there emerge two distinct cases, depending on whether there are any significant obstacles between the two of them: Line-of-sight (LOS) and Non-line-of-sight (NLOS).

3.2.1 Manhattan grid

In order to determine whether a given link is a LOS or NLOS link, we need information about the obstacles present in the path between the two. In our case, we don't consider objects like cars and people explicitly, but rather account for all such minor objects and reflections they might create with a stochastic model (see 3.3). Buildings, on the other hand, represent such massive, nigh-impenetrable objects that we must contemplate them concretely.

The preferred method mentioned in the METIS deliverables is the use of a "Manhattan-like" grid, meaning a city-layout comprised of rectangular blocks criss-crossed by wide streets. To determine both the size and the overall layout of our Manhattan Grid, we again turn to the extensive work done by METIS. The measurements with which their relevant models were tested were run in Madrid, with a grid of around 500 meters of both length and width. We homogenized the scenario by having exclusively square blocks, but maintained both the street width and the general dimensions.

Parameter	**Value**
Grid Dimensions	500 m $\times$ 500 m
Block Width	110 m
Block Length	110 m
Street Width	20 m

Table 3.1: Manhattan grid parameters

The introduction of an explicit grid raises the issue of the positioning of our UEs again. Having scattered them in a Poisson point process (see 3.1), some inevitably now find themselves inside a building and not on the street, as is necessary for our O2O simulations.

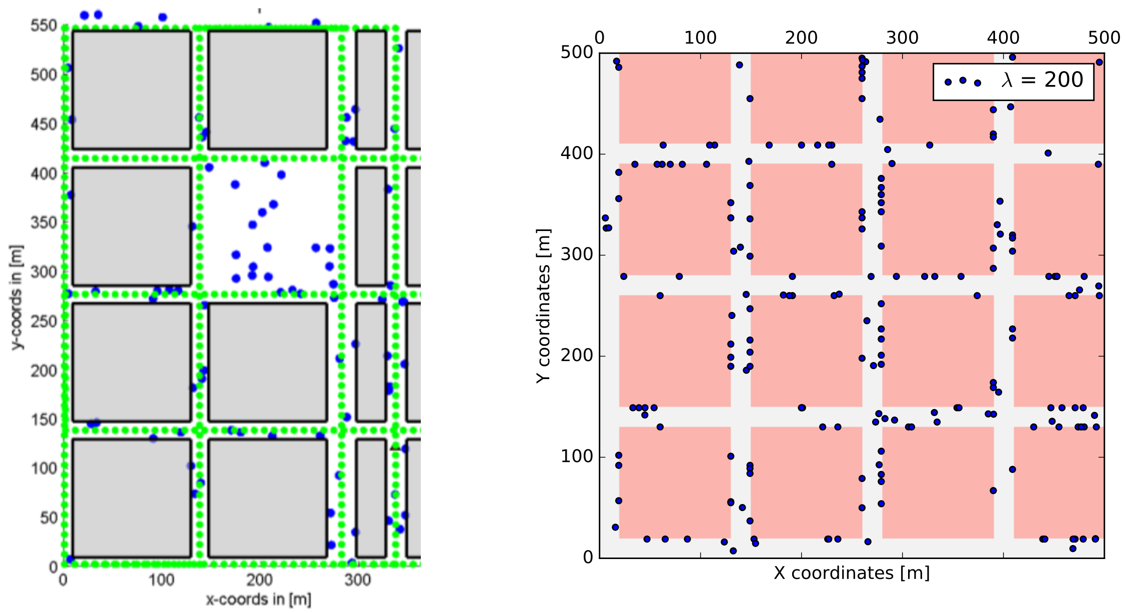

(a) Madrid grid [Mw15] (b) Own implementation, including moved UEs

Figure 3.2: Comparison between two Manhattan Grids

We overcome this obstacle by simply finding the shortest route from the position inside a block to the street: as the UE position is random, so too is the route taken. Thus we avoid completely discarding the randomness of their positioning. The results can be seen in figure 3.2b and compared to the actual city grid used for METIS measurements (figure 3.2a).

With a Manhattan-like layout at the ready, questions about whether a link has LOS or not become much easier to answer.

3.2.2 Line-of-sight

The overall model for pathloss used by [Mw15] is derived specifically from the one presented in [Rep09] by the ITU (International Telecommunication Union) and covers a wide frequency range (0.8 to 60 GHz). Distances between 10 and 500 meters are thus defined by two distinct equations, depending on whether the distance between the two points is greater than a certain "breakpoint distance". The distance d'_{BP} in question is defined by

$$d'_{BP} = 0.87 \exp\left(- \frac{log_{10}\left(\frac{f_c}{1GHz}\right)}{0.65} \right) \frac{4\, h'_{BS} h'_{UE}}{\lambda_{WL}} , \tag{3.2}$$

with h'_{BS} as the effective height of the Base Station and h'_{UE} the effective height of the UE, with "effective" denoting adjusting for environment height h_e. The λ_{WL} is the wavelength of the signal, which is calculated from the center frequency f_c and the speed of light c. It must be mentioned that for our transmissions, the height of both the origin and destination device will be identical more often than not, due to cluster connections being D2D links.

An additional "pathloss offset" PL_1 is defined in order to bring the model in agreement with the control measurements performed by METIS and is designed to account for elements like multipath fading.

$$PL_{1|dB} = -1.38\,\log_{10}\left(\frac{f_c}{1Ghz}\right) + 3.34 \tag{3.3}$$

The actual pathloss equations are given as a function of distance d by

$$PL_{LOS}(d)_{|dB} = 10\,n_1\,\log_{10}\left(\frac{d}{1m}\right) + 28.0 + 20\log_{10}\left(\frac{f_c}{1GHz}\right) + PL_{1|dB} \tag{3.4}$$

for $10\,m < d \leq d'_{BP}$ and

$$PL_{LOS}(d)_{|dB} = 10\,n_2\,\log_{10}\left(\frac{d}{d'_{BP}}\right) + PL_{LOS}(d'_{BP})_{|dB} \tag{3.5}$$

for $d'_{BP} < d \leq 500m$ (compare with [Mw15]). The parameters $n_1 = 2.2$ and $n_2 = 4.0$ are the power decay constant on both sides of the break point distance.

3.2.3 Non-line-of-sight

Most of the connections available to a given UE will be NLOS links. These happen whenever the UE tries to communicate with a device that is not on its same street and thus the signal has to travel a more convoluted way in order to be received. METIS defers explicitly to the final channel models, created by WINNER+ (Wireless World Initiative New Radio+) in [HSK$^+$10]. WINNER+ is a private consortium looking to further develop the IMT-A (International Mobile Telecommunications-Advanced) standards.

The conceptual NLOS model in itself comes from an even earlier work, [MKJH09], which details the relevant parameters for NLOS communication in an urban setting. In these cases, the corners resulting from intersecting streets act as relay nodes for the signal. [MKJH09] designates two distances needed to calculate the pathloss in this route, see figure 3.3b, where d_1 is distance from relay node to BS and d_2 to the UE. As was the case for the difference in heights between UE and BS, seeing as the links we are investigating are D2D, there is no real clear theoretical distinction between d_1 and d_2. However, we keep the distinction intact (with the same emitter/receiver relation) owing to the fact that "[t]hough the pathloss between BS and UE must be the same regardless of the direction of signal transmission due to reciprocity, the pathloss *models* do not necessarily hold the reciprocity" ([Mw15]).

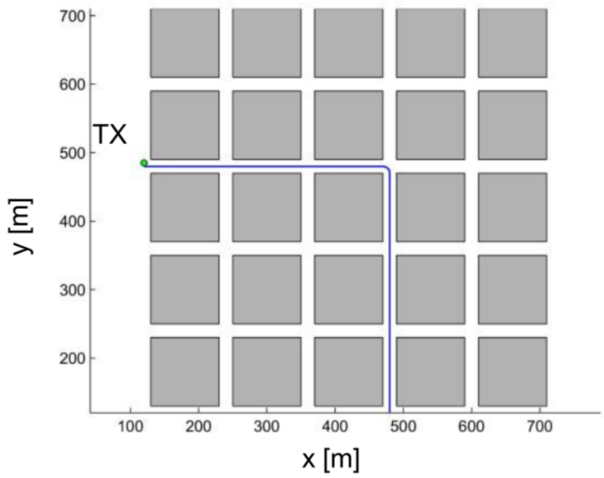

(a) Node Relay example [Mw15]

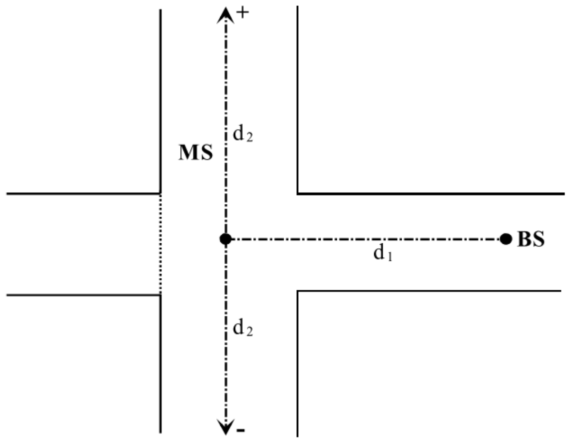

(b) Distances d_1 and d_2 [MKJH09]

Figure 3.3: Calculation of NLOS path

Thus, the formula for pathloss in the studied case is presented in [Mw15] after a small simplification and again featuring the "pathloss offset" (equation 3.3) mentioned in 3.2.2:

$$\begin{aligned} PL_{NLOS}(d_1, d_2)_{|dB} = & PL_{LOS}(d_1)_{|dB} + 17.9 - 12.5\, n_j \\ & + 10\, n_j \log_{10}\left(\frac{d_2}{1m}\right) + 3\log_{10}\left(\frac{f_c}{1GHz}\right) + PL_{1|dB}, \end{aligned} \tag{3.6}$$

where n_j is a power decay constant calculated as

$$n_j = \max(2.8 - 0.0024\, d_1,\ 1.84). \tag{3.7}$$

In a rectangular Manhattan grid such as ours, a only two intersections are needed as relays in order to connect any two given points on the grid. An algorithm was thus created to calculate the shortest possible distance between the two devices using a maximum of two intersections. We take the shortest possible route because the signal spreads omnidirectionally. An example of a calculated route between two points can be seen in figure 3.4.

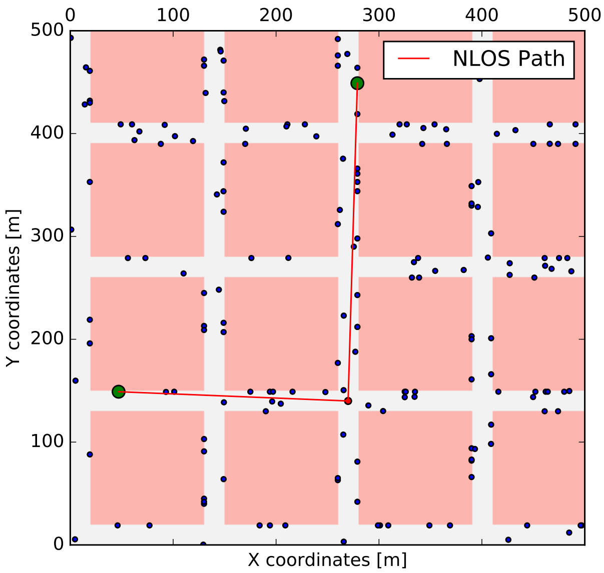

Figure 3.4: Visualization of NLOS path with intersection acting as relay node

3.3 Shadow fading

As mentioned in 3.2.1, Shadow Fading - meaning the effects on the signal caused by smaller obstacles - as well as the reflections they create are modelled through a stochastic model. This type of fluctuation, called "Shadow Fading" or "long-term fading" is often realized through a Gaussian distribution in the logarithmic scale (also called a log-normal distribution), as asserted in [FSA04] and shown below in its probability density function. In our case, we followed METIS specifications and set $\mu_{L_s} = 0$ and $\sigma_{L_s} = 7$dB.

$$p(L_s) = \frac{1}{\sigma_{L_s}\sqrt{2\pi}} \exp\left(- \frac{(L_s - \mu_{L_s})^2}{2\,\sigma_{L_s}^2} \right) \tag{3.8}$$

While any given point is distributed randomly along the normal distribution, completely random and uncorrelated shadow fading variables make little sense when one considers that the effects of any given set of obstacles won't change much in the space of a couple of meters. In order to account for the necessary correlation that these shadow fading variables experience, a normalized autocorrelation function is introduced, both in [FSA04] and [Mw15], with a decorrelation value suggested by METIS $d_{corr} = 8m$.

$$R(\Delta x) = \exp\left(- \frac{|\Delta x|}{d_{corr}} \ln(2) \right) \tag{3.9}$$

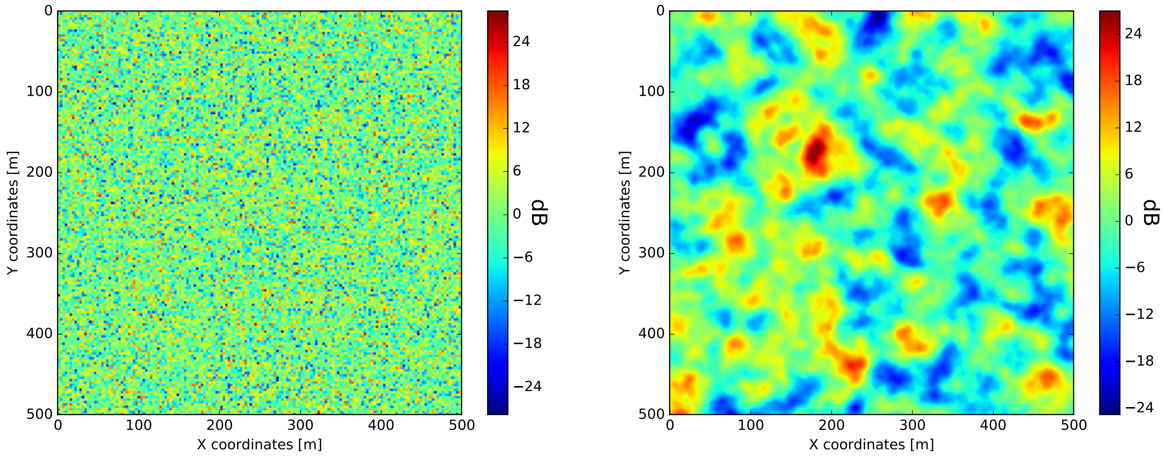

(a) Uncorrelated Shadow Fading values (b) Correlated Shadow Fading values

Figure 3.5: Shadow Fading values before and after correlation adjustment

After generating the shadow fading variables with equation 3.8 and the autocorrelation coefficients with equation 3.9, both matrices are convoluted to generate the correlated values. Convolution does not alter the underlying distribution, but it does elicit a correction of the mean and standard deviation (compare with [FSA04]) in order to return it to the values of the original Gaussian distribution. Our realization is shown below, both before and after the aforementioned correction for spatial correlation.

These shadow fading fading values are added to the pathloss values in order to fully account for all the obstacles in the way of the signal between two devices. The complete attenuation value then determines the received signal strength at the target device.

A summary of the relevant parameters utilized for the calculation of the pathloss can be seen in table 3.2

Parameter	Value
Mean point density λ	$50 - 1000$
Center Frequency f_c	$2\,\mathrm{GHz}$
Wavelength λ_{WL}	$0.15\,\mathrm{m}$
Speed of light c	$3 \cdot 10^8\,\frac{\mathrm{m}}{\mathrm{s}}$
Height of UE h_{UE}	$1.5\,\mathrm{m}$
Height of BS h_{BS}	$10\,\mathrm{m}$
Environment height h_e	$1\,\mathrm{m}$
Power decay constant n_1	2.2
Power decay constant n_2	4.0
Shadow Fading mean μ_{L_s}	0
Shadow Fading standard deviation σ_{L_s}	$7\,\mathrm{dB}$
Decorrelation distance d_{corr}	$8\,\mathrm{m}$

Table 3.2: Parameters relevant for pathloss calculation

3.4 Random access procedure and interference

When reducing the load that the eNB experiences as a result of an increase in the amount of devices connecting to it by means of clustering, a large amount of the load is simply transferred to the cluster heads. These have then to take up the functions of the eNB in terms of implementing a random access procedure through which to service the UEs connecting to it. As mentioned in section 2.2, we contemplate an explicit separation of resources for normal BS to UE communication and D2D communication, putting further constraints on the ability of the cluster head to detect and separate signals using the same resource blocks. In order to best model these kinds of phenomena, the author utilized simulations developed by his supervisor, M.Sc. Mikhail Vilgelm, that were kindly put at his disposition for this work.

Firstly, a Poisson process is used in modeling the arrival of packages proceeding from connected UEs to the appropriate cluster head. This Poisson arrival process is analogous to that shown in equation 3.1 and yields the amount of packages arrived at a certain point in time instead of points in an area. The arrival rate, λ_A was set by recommendation of the author's supervisor to a level where the derivative of the throughput with respect to the arrival rate is positive, at $\lambda_A = 1.5$.

The requests are generated at the given rate and broadcast with a set transmission power P_{Tx}. Although there are many proposals for power control schemes in D2D communications, such as [EMIA13], [WHS12b] or [LLA15], due to there being so many varied schemes and them adding such complexity to the simulation, it was decided that power control would not be part of the scope of this work. As in [KK14b], we decide to use $P_{Tx} = 23\,\mathrm{dBm}$ for our simulation, which is incidentally the power level used for coverage issue identification in [3rd12] and the maximum transmit power for public safety defined in [3rd14], both by the 3GPP.

The power is then affected by the appropriate attenuation at the spot of the receiving device (see section 3.2) and the resulting power is the received power $P_{Rx|dBm} = P_{Tx|dBm} - PL_{|dB}$. In order to assess whether a given signal has reached the cluster head with enough power to be detected, we look at the SINR (Signal-to-Interference-and-Noise-Ratio) of the transmission. For the calculation of the noise we use a thermal noise density $N_0 = -174\,\frac{\mathrm{dBm}}{\mathrm{Hz}}$, UE receiver noise figure $NF_{UE} = 9\,\mathrm{dB}$ and system bandwidth $W = 10\,\mathrm{MHz}$, as defined in [3rd12].

The incoming requests are checked for additional interference coming from other requests using the same preamble, both within and without the cluster. The received power I of those interfering signals at the cluster head are added and that total added to the noise power P_N to finally calculate the SINR, see equation 3.10. As mentioned earlier, the available preambles for transmission of a D2D link are drawn from the overall pool of preambles available in LTE-A. As mentioned in [Cox12], 64 preambles are available to the cell, only 6 of which are available for D2D communication. This is to allow normal cellular UEs to experience an acceptable QoS (Quality of Service), while still allowing other devices access to the network.

$$SINR = \frac{P_{Rx}}{I + P_N} \tag{3.10}$$

As to the minimum SINR needed to connect to the cluster head, a threshold of $SINR_{thr} = 10\,\mathrm{dB}$ was chosen within the range presented in [3Gp09] for the minimum ratio necessary to transmit with "an acceptably low BER (Bit Error Rate) in the output data." Those requests under the threshold will be filtered out before they are dealt with by the cluster head. Please note that although they are not counted towards successful requests, they will count towards interference values of other requests that may or may not clear the threshold.

Finally, requests clearing the threshold will be handled by the cluster head, who will then check for intra-cluster preamble collisions and give feedback, negative or positive, to the UEs. For simplicity's sake, feedback is assumed to arrive safely back at the UE; positive feedback elicits no action from the original transmitter. Upon reception of negative feedback, on the other hand, the UE "backs off" for an amount of time before attempting the connection once again at a later point in time. If the device is told to back off 20 times, it assumes the connection has failed completely and will not try again until another packet is generated at that UE.

Readers can find a summary of all used parameters for this stage on table 3.3.

Parameter	**Value**
Request arrival rate λ_A	1.5
Transmission power P_{Tx}	23 dBm
Noise density N_0	$-174\,\frac{\text{dBm}}{\text{Hz}}$
UE receiver noise figure NF_{UE}	9 dB
BS receiver noise figure NF_{BS}	5 dB
System Bandwidth W	10 MHz
Number of total LTE-A preambles	64
Number of preambles available for D2D communication	6
SINR threshold $SINR_{thr}$	10dB

Table 3.3: Parameters relevant for random access and interference

The last piece of the puzzle is, of course, the actual mapping of UEs to cluster heads. These are fed into the random access and interference simulation by the clustering algorithms.

3.5 Clustering Algorithms

Chapter 4

Conclusions and Outlook

The thesis is concluded here. The considered problem is repeated. The contribution of this work is highlighted and the results are recapitulated. Remaining questions are stated and ideas for future work are expressed.

Appendix A

The appendix may contain some listings of source code that has been used for simulations, extensive proofs or any other things that are strongly related to the thesis but not of immediate interest to the reader.

Appendix B

Notation und Abkürzungen

This chapter contains tables where all abbreviations and other notations like mathematical placeholders used in the thesis are listed.

BS	Base Station
CH	Cluster Head
D2D	device to device
eNodeB	evolved Node B or E-UTRAN Node B
IMT-A	International Mobile Telecommunications-Advanced
IoT	Internet of Things
ITU	International Telecommunication Union
LOS	Line-of-Sight
LTE	Long Term Evolution
MCS	Modulation and Coding Scheme
METIS	Mobile and wireless communications Enablers for the Twenty-twenty Information Socie
MTC	Machine Type Communication
NLOS	Non-Line-of-Sight
OFDM	Orthogonal Frequency Division Multiplexing
O2I	Outside-to-Inside
O2O	Outisde-to-Outside
PDCCH	Physical Downlink Control Channel
PDSCH	Physical Downlink Shared Channel
PPP	Poisson Point Process
PRB	Physical Resource Block
PUCCH	Physical Uplink Control Channel
PUSCH	Physical Uplink Shared Channel
QoS	Quality of Service
RA	Random Access
RACH	Random Access Channel
SINR	Signal-to-Interference-and-Noise-Ratio
SNR	Signal-to-Noise-Ratio
SR	Scheduling Request
UE	User Equipment
WINNER+	Wireless World Initiative New Radio+
WSN	Wireless Sensor Network
3GPP	Third Generation Partership Project

List of Figures

List of Tables

Bibliography

[3Gp09] 3Gpp. TR 136 942 - V8.1.0 - LTE; Evolved Universal Terrestrial Radio Access (E-UTRA); Radio Frequency (RF) system scenarios (3GPP TR 36.942 version 8.1.0 Release 8). 0:0–84, 2009.

[3rd11] 3rd Generation Partnership Project;. Ran Improvements for Machine-type Communications [RP-100330], 2011.

[3rd12] 3rd Generation Partnership Project;. Evolved Universal Terrestrial Radio Acces; LTE Coverage Enhancements (Release 11) [36-824]. 0(Release 11), 2012.

[3rd14] 3rd Generation Partnership Project;. Study on LTE Device to Device Proximity Services; Radio Aspects (Release 12) [36843-c01], 2014.

[ATN14] M Mehdi Afsar and Mohammad H Tayarani-N. Clustering in sensor networks: A literature survey. *Journal of Network and Computer Applications*, 46:198–226, 2014.

[Cox12] Christopher Cox. *AN INTRODUCTION TO LTE: LTE, LTE-Advance, SAE and 4G Mobile Communicatios.* 2012.

[EMIA13] M Cenk Erturk, Sayandev Mukherjee, Hiroyuki Ishii, and Huseyin Arslan. Distributions of transmit power and SINR in device-to-device networks. *IEEE Communications Letters*, 17(2):273–276, 2013.

[FSA04] Ingo Forkel, Marc Schinnenburg, and Markus Ang. Generation of two-dimensional correlated shadowing for mobile radio network simulation. *WPMC, sep*, (February):10–14, 2004.

[HSK+10] Petteri Heino, Essi Suikkanen, Esa Kunnari, Juha Meinilä, Pekka Kyösti, Lassi Hentilä, Tommi Jämsä, and Milan Narandžić. D5.3: WINNER+ Final Channel Models. 1(107):107, 2010.

[JYZ09] Congfeng Jiang, Daomin Yuan, and Yinghui Zhao. Towards Clustering Algorithms in Wireless Sensor Networks-A Survey. *2009 IEEE Wireless Communications and Networking Conference (WCNC2009)*, pages 1–6, 2009.

[Kee] Holger Paul Keeler. Studying the SINR process of the typical user in Poisson networks by using its factorial moment measures . pages 1–27.

[Kee16] Paul Keeler. Notes on the Poisson point process. pages 1–33, 2016.

[KK14a] Markus Klugel and Wolfgang Kellerer. Introduction of an efficiency metric for device-to-device communication in cellular networks. *IEEE Vehicular Technology Conference*, 2014.

[KK14b] Markus Klügel and Wolfgang Kellerer. On the feasibility of frequency reuse and spatial occupation in wireless device-to-device networks. *2014 IEEE International Black Sea Conference on Communications and Networking, BlackSeaCom 2014*, pages 154–159, 2014.

[LAAZ14] A Laya, L Alonso, and J Alonso-Zarate. Is the Random Access Channel of {{}LTE{}} and {{}LTE-A{}} Suitable for {{}M2M{}} Communications? A Survey of Alternatives. 16(1):4–16, 2014.

[LLA15] Namyoon Lee, Xingqin Lin, and Jeffrey G Andrews. Power Control for D2D Underlaid Cellular Networks: Modeling, Algorithms and Analysis. *IEEE Journal on Selected Areas in Communications*, 33(1):1–12, 2015.

[LQL13] Ying Liao, Huan Qi, and Weiqun Li. Load-balanced clustering algorithm with distributed self-organization for wireless sensor networks. *IEEE Sensors Journal*, 13(5):1498–1506, 2013.

[LWW+14] Andres Laya, Kun Wang, Ashraf Awadelkarim Widaa, Jesus Alonso-Zarate, Jan Markendahl, and Luis Alonso. Device-to-device communications and small cells: Enabling spectrum reuse for dense networks. *IEEE Wireless Communications*, 21(4):98–105, 2014.

[MKJH09] Juha Meinilä, Pekka Kyösti, Tommi Jämsä, and Lassi Hentilä. WINNER II Channel Models. *Radio Technologies and Concepts for IMT-Advanced*, 1(82):39–92, 2009.

[Mw15] Mobile and wireless communications Enablers for the Twenty-twenty Information Society. Deliverable D1.4 METIS Channel Models. 2015.

[NXW11] D Niyato, Lu Xiao, and Ping Wang. Machine-to-machine communications for home energy management system in smart grid. *Communications Magazine, IEEE*, 49(4):53–59, 2011.

[PCZZ16] Michele Polese, Marco Centenaro, Andrea Zanella, and Michele Zorzi. On the Evaluation of LTE Random Access Channel Overload in a Smart City Scenario. 3, 2016.

[RCCM15] Andre Riker, Eduardo Cerqueira, Marilia Curado, and Edmundo Monteiro. A Two-Tier Adaptive Data Aggregation Approach for M2M Group-Communication. *IEEE Sensors Journal*, 16(c):1, 2015.

[Rep09] Report ITU-R M.2135-1. Guidelines for evaluation of radio interface technologies for IMTadvanced. *Evaluation*, 93(3), 2009.

[SOIJ15] H Shariatmadari, P Osti, S Iraji, and R Jäntti. Data Aggregation in Capillary Networks for Machine-to-Machine Communications. *Proc. IEEE Personal, Indoor and Mobile Radio Communications (PIMRC) – Workshop on M2M Communications: Challenges, Solutions and Applications*, pages 1100–1105, 2015.

[WHS12a] Shih-en Wei, Hung-yun Hsieh, and Hsuan-jung Su. Enabling Dense Machine-to-Machine Communications through Interference-Controlled Clustering. pages 774–779, 2012.

[WHS12b] Shih-en Wei, Hung-yun Hsieh, and Hsuan-jung Su. Joint Optimization of Cluster Formation and Power Control. pages 5512–5518, 2012.

[WSH+13] Sen Hung Wang, Hsuan Jung Su, Hung Yun Hsieh, Shu Ping Yeh, and Minnie Ho. Random access design for clustered wireless machine to machine networks. *2013 1st International Black Sea Conference on Communications and Networking, BlackSeaCom 2013*, pages 107–111, 2013.